

Concerning the $\text{Ca}_{2-x}\text{Mg}_x\text{Tt}$ Systems, $\text{Tt} = \text{Sn}, \text{Pb}$

Ashok K. Ganguli, Arnold M. Guloy, and John D. Corbett¹

Ames Laboratory—DOE² and Department of Chemistry, Iowa State University, Ames, Iowa 50011

Received January 11, 2000; in revised form March 7, 2000; accepted March 10, 2000

The $\text{Ca}_2\text{Tt}-\text{Mg}_2\text{Tt}$ systems for tetrel $\text{Tt} = \text{Sn}, \text{Pb}$ each contain a single $\text{Ca}_{2-x}\text{Mg}_x\text{Tt}$ phase with the Co_2Si structure ($Pnma$) over $0 \leq x \leq 1$, beyond which Mg_2Tt (inverse CaF_2 -type, $x = 2$) appear. At $x = 1$, Mg occupies the unique position in the tricapped trigonal prisms (TCTP) of cations about tin that is not involved in the formation of chains of edge-shared prisms, but rather it participates in interchain bonding via face-capping functions on adjoining trigonal prisms. This substitution produces notably less distortion in the TCTP units than in Ca_2Tt . Resistivity data for the tin system show changes from a semiconductor for Ca_2Sn to a poor metal at CaMgSn , $\rho \sim 180 \mu\Omega \text{ cm}$ at 240 K. Only very small and approximately temperature-independent magnetic susceptibilities are found over the same range, values that are only fractions of the standard diamagnetic core corrections. The systems behave as typical Zintl phases containing Ca^{2+} , Mg^{2+} , and Tt^{4-} oxidation states. © 2000 Academic Press

1. INTRODUCTION

Two independent investigations have led to the discovery of new relationships in the systems $\text{Ca}_{2-x}\text{Mg}_x\text{Tt}$ for the tetrels (Tt) tin and lead. Both studies started with systems close to the compositions $\text{Ca}_5\text{Tt}_3\text{Z}$ for the particular cases where Z was Mg, but both proved to be unsuccessful in producing either target. Attempts to achieve a doped version of the unknown Ca_5Sn_3 for compositions $\text{Ca}_{5-y}\text{Mg}_y\text{Sn}_3$, presumably close to a W_5Si_3 -type structure, led instead to the remarkable layered phase $\text{Ca}_{6.2}\text{Mg}_{3.8}\text{Sn}_7$ with its zig-zag chains of interconnected square planar tin units (1). Further experiments in which the active metal proportions were varied in order to establish the fixed stoichiometry of the last discovery also led to recognition that a second phase with a Co_2Si -type structure was present

¹To whom correspondence should be addressed. E-mail: jcorbett@iastate.edu.

²This research was supported by the Office of the Basic Energy Sciences, Materials Sciences Division, U.S. Department of Energy. The Ames Laboratory is operated for DOE by Iowa State University under Contract No. W-74-5-Eng-82. Accordingly, the U.S. Government retains a nonexclusive, royalty-free license to publish or reproduce the published form of the contribution, or to allow others to do so for U.S. Government purposes.

and that its lattice constants varied with magnesium content.

Other investigations of stuffed Mn_5Si_3 -type $\text{Ca}_5\text{Pb}_3\text{Z}$ systems, for which the electron-poor binary Ca_5Pb_3 is unknown, revealed that surprisingly stable ternary compounds could be formed in this structure for $\text{Z} = \text{V}-\text{Ni}$, leading to the conclusion that these Z were in effect functioning as two-electron donors (2). Attempts to extend this series to $\text{Z} = \text{Mg}$ gave instead a single-phase orthorhombic Ca_5MgPb_3 ($= \text{Ca}_{1.67}\text{Mg}_{0.33}\text{Pb}$) product with the same Co_2Si structure. Continuously varying proportions of the two active metals in this phase was again achievable.

The orthorhombic Co_2Si -type structure (3) is assigned within a wider family of PbCl_2 -type structures to a group with cell proportions in a range of about $0.83 < a/c < 0.88$. The former group includes both Ca_2Sn (4) and Ca_2Pb (5). At the other extreme, Mg_2Sn and Mg_2Pb are both members of the inverse-fluorite family (6). A single report of the formation of a different Mg_2Pb (7), possibly a Co_2Si -type (6), has not been confirmed; rather, recent evidence suggests that the assignment was in error and that the phase has a different composition and, presumably, structure (8). The Co_2Si structure type contains equal proportions of two distinctive cation sites, and so it is not surprising that the 1:1 mixed phases CaMgSn (9) and CaMgPb (10) with segregated cations are also known in the orthorhombic Ca_2Tt structure. This article concerns the $\text{Ca}_2\text{Sn}-\text{CaMgSn}$ and $\text{Ca}_2\text{Pb}-\text{CaMgPb}$ regions of these systems.

EXPERIMENTAL

The usual reaction conditions in welded Ta tubing, glovebox handling for all samples, and X-ray powder diffraction with Enraf Nonius Guinier cameras from samples tightly sealed between pieces of cellophane tape were all carried out as before (1). NIST silicon was used as an internal standard to provide accurate lattice parameters from the film data. The elements calcium (4–9's, Applied Physics Lab or Ames Lab triply distilled), magnesium (4–9's, Ames Lab), tin (4–9's, Baker, clean on fusion), and lead (6–9's, Cominco Products, electrolytic bar) were used



to synthesize Ca_{2-x}Mg_xTl (Tl = Sn, Pb) samples. The tin reactions were generally equilibrated at 1030°C for ~2 days and quenched to room temperature. The first lead reactions involved slow cooling from 850°C, but reactions at higher temperatures, 1050–1100°C, that were quenched or slowly cooled gave the same results. The products all seemed to melt congruently.

Magnetic susceptibilities were measured on powdered samples held between the faces of two silica rods within a container sealed under He (11). Data were collected at 3 T between 6 and 300 K on a Quantum Design MSPS SQUID magnetometer and corrected for core contributions. Resistivities were measured at 35 MHz over ~90–255 K by the “Q” method on finely powdered and sized samples diluted with chromatographic Al₂O₃. The resistivity values obtained by this method are believed to be accurate within a factor of about 3 (12).

RESULTS AND DISCUSSION

Reactions between Ca₂Sn and Mg₂Sn yielded a single phase region Ca_{2-x}Mg_xSn over the range 0 ≤ x ≤ ~1.0, i.e., terminating with CaMgSn. All powder patterns over this region contained only lines of the orthorhombic Ca₂Sn, CaMgSn structure (*Pnma*, no. 62, Z = 4) or their solid solutions, while Mg₂Sn was also present for x ≫ 1. The course of the lattice constants across the homogeneity region is shown in Fig. 1. The lattice parameters for the end

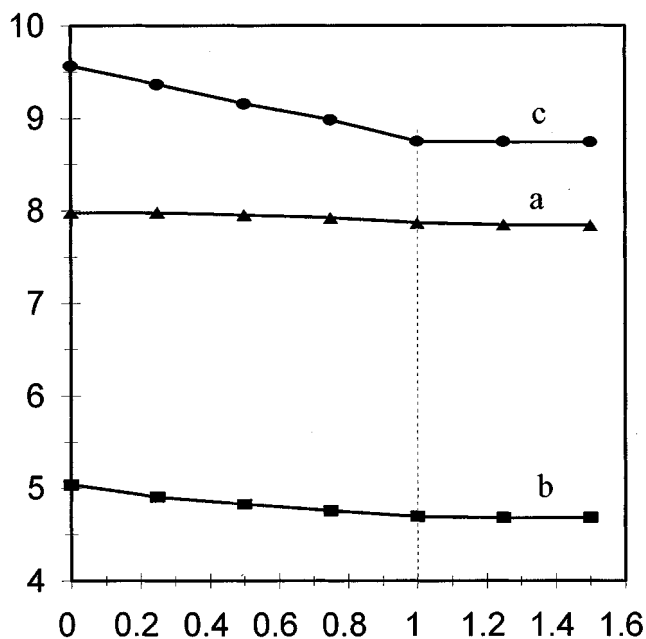


FIG. 1. Lattice constants (Å) for the orthorhombic Co₂Si-type phase (*Pnma*) of Ca_{2-x}Mg_xSn over the range 0 ≤ x ≤ 1.5. (a, ▲; b, ■; c, ●). The system is single phase only up to x = 1. Breaks in all dimensions are evident at that point, but they are most obvious in the intersheet \bar{c} direction where Mg intrudes.

TABLE 1
Lattice Parameters (Å) for Phases with Co₂Si-Type (*Pnma*) Structure and Mg₂Sn (This Work)

	a	b	c	a/c
CaMgSn	7.8731(8)	4.6941(3)	8.7538(7)	0.900
CaMgPb	7.904(4)	4.772(1)	8.880(1)	0.890
Ca ₂ Sn	7.981(2)	5.043(1)	9.566(2)	0.834
Ca ₂ Pb	8.0720(4)	5.100(1)	9.647(1)	0.837
Mg ₂ Sn	6.7645(3)			

points in this and the lead system are given in Table 1. Our data for Ca₂Sn (4), CaMgSn (9), and Mg₂Sn (13) are all within 1σ of previous reports. The character of the changes across this homogeneous region can be understood better by reference to the structure of CaMgSn (9) shown in Fig. 2. This is built from tricapped trigonal prisms of cations about each Sn (black) (or Pb) that share basal faces along *b*, the projection axis. The connections in the figure highlight these prisms, while the actual bonds between the cations and Sn (Pb) within the prisms are not marked. Each trigonal prism shares two Ca–Ca side edges (larger open spheres) to generate infinite zig-zag chains (darkened and horizontal in Fig. 2) that run parallel to \bar{a} or which are actually sheets of

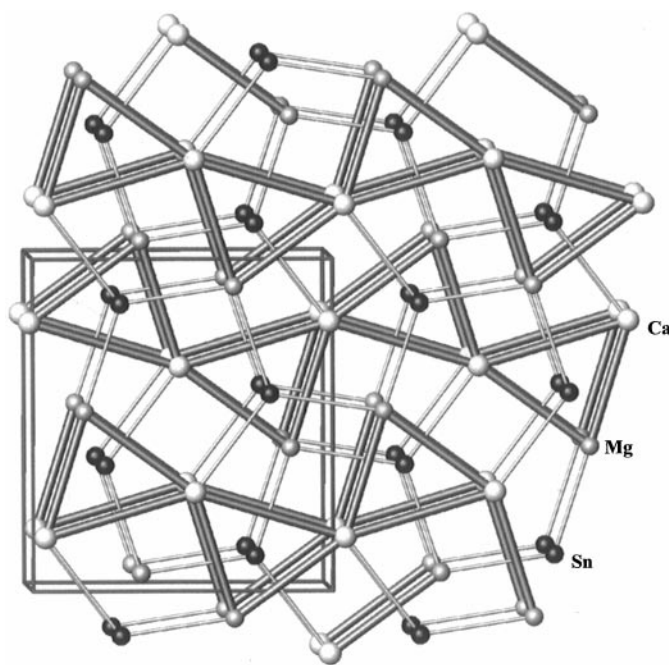


FIG. 2. Structure of CaMgSn (9) viewed in a near-projection along the short *b* axis. Large white and small darker spheres represent Ca and Mg, respectively, while black spheres are Sn. Shaded trigonal prisms emphasize the zig-zag chains of trigonal prismatic columns that share calcium atoms along \bar{a} (horizontal). These alternate by *b*/2 in their stacking along \bar{c} (vertical). Bonds are marked between tin and only the augmenting face-capping (2 Mg, 1 Ca) cations that interconnect the chains.

shared prisms that lie along the projection axis and normal to \vec{c} (vertical).

Note that this construction leaves the magnesium (small, darker) atoms on the unique, unshared edges of the prisms. In addition, the sheets of trigonal prisms normal to \vec{c} are positioned such that adjacent ones are displaced by $b/2$. This places the Mg and Ca atoms on the same mirror planes as Sn (Pb) in adjoining sheets, so that the former serve the familiar function of capping the rectangular faces of the prisms, two by Mg, one by Ca, to complete the familiar CN9 tricapped trigonal prism (TCTP) about tin (lead). These bridges also serve to "glue" the sheets together. The unique substitution of Mg at the unshared edge of the trigonal prism not only gives reason for the dimensional behavior seen in Fig. 1 but also produces a less distorted structure. In Ca_2Sn (4), the tin is notably off-center in the trigonal prism, with distance ranges of 0.53 Å (3.13–3.70 Å) to the prismatic cations and 0.23 Å to the face-capping cations, in each case the tetrel element lying closer to the cations that become the Mg atom in CaMgSn . [Ca_2Pb is somewhat more extreme (10).] In general, CaMgSn exhibits more symmetric bonding even considering the Mg substitution. The tin is more nearly central in the distorted trigonal prism and the angles at tin between bonds to the face-capping atoms range only between 117° and 124°. The role of magnesium in defining these sheet structures is very similar to its function in the novel $\text{Ca}_{6.2}\text{Mg}_{3.8}\text{Ca}_7$ (1).

The lead system was investigated less extensively. Lattice dimensions of the end members Ca_2Pb and CaMgPb agree very well with literature data within the precision of the reports (4, 10), although lattice constants in another report on Ca_2Pb (5) are 0.03–0.04 Å smaller, suggesting impurity problems. The intermediate $\text{Ca}_{1.67}\text{Mg}_{0.33}\text{Pb}$ gave lattice constants that deviated by 0, 0.067, and 0.077 Å from a linear interpolation between the end members (Vegard's rule), the last two amounting to differences of only 1.4% and 0.8%, respectively. The composition $\text{Ca}_{1.67}\text{Sr}_{0.33}\text{Pb}$ also occurs in this structure, the strontium probably substituting on the shared sites along the chain. Incidentally, there is no fourth capping atom about the trigonal prisms in any of the present structures, contrasting with a seeming generality that has been applied to the Co_2Si -type structure (14).

Resistivities of Ca_2Sn , $\text{Ca}_{1.50}\text{Mg}_{0.5}\text{Sn}$, and CaMgSn show a regular progression from a semiconductor to a poor metal. The resistivities found ($\mu\Omega\text{ cm}$) at $\sim 240\text{ K}$ and the temperature coefficients therebelow are as follows for $x = 0$, 1050, -0.28% ; for $x = 0.50$, 400, -0.32% ; and for $x = 1.0$, 180, $+0.27\%$. These changes may be associated with the closer approach of the tin anions at $x = 1$. These separations remain large, 4.66–4.76 Å, but each is about 0.4 Å less than in Ca_2Sn . Of course, there may be subtle doping effects, too. The number of carriers in CaMgSn is still low, and the continued formulation of it as a Zintl phase with oxidation states $\text{Ca}^{+2}\text{Mg}^{+2}\text{Sn}^{-4}$ is appropriate. The aver-

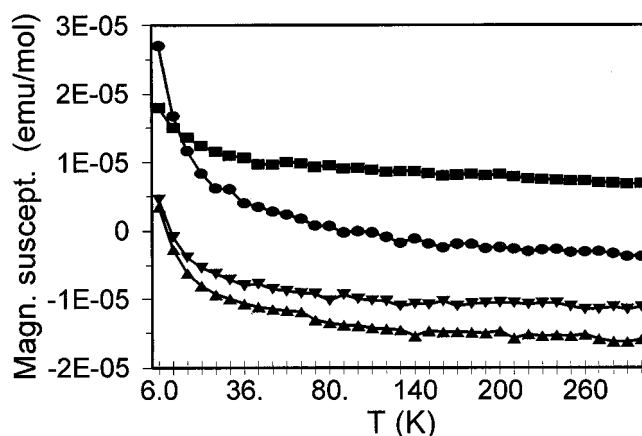


FIG. 3. Molar magnetic susceptibilities (corrected for core contributions) for $\text{Ca}_{2-x}\text{Mg}_x\text{Sn}$ samples: $x = 0$ (■), 0.25 (●), 0.5 (▼), 1 (▲).

age of five Sn–Ca distances, 3.32 Å, is comparable to 3.25 Å ($\times 6$) in CaCdSn (Fe_2P) (15), 3.37 Å among a more distorted polyhedron of eight about isolated tin atoms in $\text{Ca}_{31}\text{Sn}_{20}$ (16), and 3.33 Å for four Ca–Sn bonds in similar trigonal prisms in $\text{Ca}_{6.2}\text{Mg}_{3.8}\text{Sn}_7$ (1).

The molar magnetic susceptibilities for these systems are less informative. These are shown in Fig. 3 for, top to bottom, $x = 0$ (Ca_2Sn), 0.25, 0.5, and 1.0 (CaMgSn). The data for each are nearly temperature-independent above about 80 K, and there is a clear trend from para- to diamagnetism in this order. But the net susceptibility values are all very small, roughly 10% or less of what have been found in related polar systems with either Pauli or van Vleck behaviors. In fact, our results are only a fraction of the sum of Selwood's traditional diamagnetic core terms sum that have been applied, viz., $3.6 \times 10^{-5} \text{ emu mol}^{-1}$ for Ca_2Sn ($2\text{Ca}^{+2} + \text{Sn}^{+2}$). The correction for tin is only an approximation, and a value appropriate to Sn^{-4} , if constant, would presumably be larger and raise all of the curves shown. However, even the best of diamagnetic salts rarely yield zero values for susceptibilities after core corrections, so we are inclined to attribute these small residuals to errors in our simple procedures and to minute effects that we do not know or understand.

ACKNOWLEDGMENT

The authors are indebted to Jerome Ostenson for the magnetic data.

REFERENCES

1. A. K. Ganguli, J. D. Corbett, and M. Köckerling, *J. Am. Chem. Soc.* **120**, 1223 (1998).
2. A. M. Guloy and J. D. Corbett, *Inorg. Chem.*, to be submitted.
3. S. Geller, *Acta Crystallogr.* **8**, 83 (1955).

4. P. Eckerlin, F. Leicht, and E. Wölfel, *Z. Anorg. Allg. Chem.* **307**, 145 (1961).
5. G. Bruzzone and F. Merlo, *J. Less-Common Met.* **48**, 103 (1976).
6. P. Villars and L. D. Calvert, "Pearson's Handbook of Crystallographic Data," 2nd ed. ASM International, Metals Park, OH, 1991.
7. J. M. Elderidge, E. Miller, and K. L. Komarek, *Trans. Met. Soc. AIME* **233**, 1303 (1965).
8. N. G. Siviour and K. Ng, *Metall. Mater. Trans. B.* **25B**, 265 (1994).
9. H. Axel, B. Eisenmann, H. Schäfer, and A. Weiss, *Z. Naturforsch.* **24B**, 815 (1969).
10. B. Eisenmann, H. Schäfer, and A. Weiss, *Z. Anorg. Allg. Chem.* **391**, 241 (1972).
11. A. M. Guloy and J. D. Corbett, *Inorg. Chem.* **35**, 4669 (1996).
12. J.-T. Zhao and J. D. Corbett, *Inorg. Chem.* **34**, 378 (1995).
13. V. M. Glazou and N. N. Glagoleva, *Inorg. Mater.* **1**, 989 (1965).
14. B. G. Hyde and S. Andersson, in "Inorganic Crystal Structures," p. 212. Wiley and Sons, Toronto, Canada, 1989.
15. A. K. Ganguli and J. D. Corbett, *J. Solid State Chem.* **107**, 480 (1993).
16. A. K. Ganguli, A. M. Guloy, E. A. Leon-Escamilla, and John D. Corbett, *Inorg. Chem.* **32**, 4349 (1993).